Celal Bayar University Journal of Science

Triphenylamine-Based Solid-State Emissive Fluorene Derivative with Aggregation-Induced Emission Enhancement Characteristics

Seda Cetindere[1]*, Musa Erdoğan[2]

[1] Gebze Technical University, Department of Chemistry, Gebze, Kocaeli, Türkiye
[2] Kafkas University, Faculty of Engineering and Architecture, Department of Food Engineering, Kars, Türkiye

* sdemirer@gtu.edu.tr
* Orcid No: 0000-0001-7599-8491

Received: 16 July 2024
Accepted: 26 September 2024
DOI: 10.18466/cbayarfbe.1516889

Abstract

Aggregation-induced emission (AIE) has garnered considerable attention in recent years. Understanding the mechanisms underlying AIE phenomena is crucial. Here, we present the design and synthesis of a novel fluorene derivative (**4**) based on triphenylamine, which exhibits typical AIE properties. The structure of it was totally characterized using FT-IR, MALDI-TOF mass analysis, elemental analysis, ^{1}H, and ^{13}C NMR spectroscopy. It displayed strong solid-state emission with diverse fluorescence characteristics. The AIE property of the compound was systematically studied using photoluminescence spectroscopy, revealing a distinct yellow light-emitting phenomenon. The solid-state luminescence showed a red shift of 148 nm compared to its luminescence in dilute dimethylformamide (DMF) solutions. Moreover, photophysical characteristics, including absorption and emission spectra, as well as fluorescence lifetime, were examined using UV–vis absorption and fluorescence emission spectroscopy. Compound (**4**) exhibited superior photosensitization abilities in both solid and solution states, with a notably enhanced effect observed in the solid state compared to the solution state.

Keywords: AIE, Fluorene, Photophysical property, Solid-state emission, Triphenylamine.

1. Introduction

Organic luminescent materials have garnered significant attention in recent decades due to their potential applications in organic electronics [1], optoelectronics [2], bio/chemosensors [3-4], and bioimaging [5-6]. Typically, these compounds are required to function effectively in solid-states [7-8]. This preference arises because once they aggregate in the solid-state, their fluorescence often diminishes rapidly or even fully quenches due to aggregation-caused quenching (ACQ) [9-10]. Various compounds, such as silole, triphenylethene, and triarylamine derivatives, have been synthesized and studied extensively for their ACQ behavior [11-12]. However, the notorious ACQ phenomenon severely limits the emission efficiency of aggregates, posing a significant challenge in the practical application of luminescent materials [13-14]. Luckily, Tang and colleagues discovered an AIE phenomenon in 2001, which stands in direct contrast to ACQ [15]. Materials exhibiting AIE emit efficiently in aggregated or solid states. This discovery has revolutionized the field by enabling the effective application of fluorescent materials. Leveraging the beneficial AIE effect, researchers have explored and developed optoelectronic devices [16], fluorescence sensor systems [17], and optical waveguides [18-21], all capable of efficient solid-state emission. The discovery and understanding of AIE have thus opened new avenues for creating more effective luminescent materials that perform better in real-world applications.

Fluorene, also known as 9*H*-fluorene (1), is a chemical compound represented by the formula $(C_6H_4)_2CH_2$ (Figure 1). This organic substance forms white crystals that emit a purple fluorescence, hence its name derived from this characteristic [22]. Fluorene-based dyes have become integral in various technologies due to their unique properties. These compounds feature a flat biphenyl structure with an extensive π-conjugated system, offering advantages such as solubility, distinct photophysical characteristics, and ease of modification [23-25]. As a result, fluorene derivatives have been extensively studied and developed into probes for applications in molecular dynamics and bioimaging,

spanning monomers, polymers, and dendrimers. The synthesis and potential applications of fluorene derivatives have garnered significant attention, establishing fluorene-based research as a prominent field in recent years [22]. These derivatives play crucial roles in materials science, finding widespread use in optical and 3D data storage [26], organic light-emitting devices [27], dye-sensitized solar cells [28], and nonlinear optical devices for telecommunications [22]. Similarly, the triphenylamine (TPA) nucleus holds considerable importance in materials science due to its advantageous thermal, electrochemical, photoelectric, and photophysical properties [29]. Organic systems incorporating the TPA donor structure are known for their notable photophysical and optical attributes, such as redox activity, efficient hole-conduction, high electron mobility, stability, solubility, two-photon absorption capability, high photoluminescent efficiency, and excellent optoelectronic characteristics [30]. Hence, the TPA scaffold is frequently favored as the electron-donor unit in organic-based materials.

In this study, a novel fluorene derivative incorporating a TPA moiety (**4**) was intentionally designed and synthesized, as illustrated in Scheme 1. The synthesis process and the detailed characterization of this luminescent compound are extensively documented. Furthermore, the photophysical properties of the compound have been thoroughly investigated. Notably, it demonstrates outstanding characteristics associated with AIE. Moreover, the solid-state form of compound (**4**) exhibits significantly enhanced fluorescence compared to its solution state.

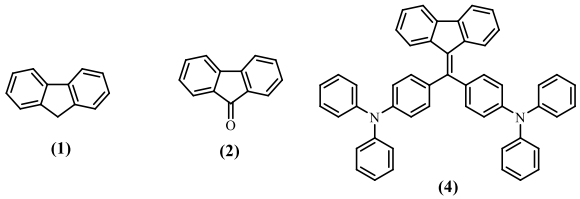

Figure 1. Molecular structures of 9*H*-fluorene (**1**), 9*H*-fluoren-9-one (**2**), and 4,4'-((9*H*-fluoren-9-ylidene) methylene)bis(*N*,*N*-diphenylaniline) (**4**)

2. Experimental

2.1. Materials and equipment

The chemicals used for synthesis were employed without further purification unless otherwise specified. We used chemical substances bought from commercial sources and deuterated solvent $CDCl_3$ for conducting NMR spectroscopy. All reactions were conducted under an argon atmosphere. The progress of the reactions was monitored using thin-layer chromatography (TLC) plates coated with silica gel. Purification of compounds were done by using column chromatography with powdered silica gel. The IR spectrum was acquired using a Perkin Elmer Spectrum 100 FT-IR spectrophotometer. Mass spectra were acquired on a Bruker Daltonics Microflex mass spectrometer. NMR spectra were recorded in $CDCl_3$ solutions using a Varian 500 MHz spectrometer. Absorption spectra were measured on a Shimadzu 2101 UV spectrophotometer in the UV–Visible region. Emission and excitation spectra were obtained using a Varian Eclipse spectrofluorometer. Fluorescence lifetimes were measured with a Horiba- Jobin-Yvon-SPEX Fluorolog 3-2iHR instrument.

2.2. Synthesis of 4,4'-((9*H*-fluoren-9-ylidene) methylene)bis(*N*,*N*-diphenylaniline), Compound (4)

The compound 9-(dibromomethylene)-9*H*-fluorene (**3**) was synthesized from 9*H*-fluoren-9-one (**2**) according to the literature [31]. To prepare compound (**4**), 500 mg (1.49 mmol) of compound (**3**) was reacted with $Pd(PPh_3)_4$ (47 mg, 0.044 mmol) and dissolved in 30 mL of DME (dimethoxyethane) in a 100 mL flask. A solution containing 4-(diphenylamino)phenylboronic acid (903 mg, 3.12 mmol) and Na_2CO_3 (473 mg, 4.46 mmol) in degassed water (15 mL) was then added to the flask. The mixture was heated under reflux for 24 hours. Once the reaction finished, the mixture was treated tree times with 50 mL ethyl acetate. The organic layers were combined and filtered on Na_2SO_4, and then concentrated under low pressure. Crude product underwent purification via column chromatography on silica gel using a solvent mixture consisting of 10% ethyl acetate and n-hexane. The resulting solid was recrystallized from a mixture of CH_2Cl_2/n-hexane (9:1), yielding compound (**4**) as yellow solid, with a yield of 970 mg (98%). It exhibited a melting point of 220°C. Elemental analysis showed the following composition in wt.-% for $C_{50}H_{36}N_2$ (calculated): C 90.33%, H 5.46%, N 4.21%. The experimental values were found to be C 90.26%, H 5.33%, N 4.15%, indicating good agreement with the calculated values. Spectral data for compound (4) included: FT-IR peaks at vmax (cm^{-1}): 3055, 3036, 1586, 1492, 1441, 1315, 1273, 751, 695. Mass spectrometry (MALDI-TOF) showed an m/z value of 664.206 [M+]. ^1H NMR spectrum (in $CDCl_3$) displayed peaks at δ ppm: 7.74 (d, J = 7.5 Hz, 2H), 7.34-7.19 (m, 32H), 6.95 (m, 2H). ^{13}C NMR spectrum (in $CDCl_3$) showed peaks at δ ppm: 148.08, 147.41, 131.56, 129.38, 124.94, 124.63, 123.40, 122.48, 119.22. These data collectively characterize the synthesized compound (**4**), confirming its structure and purity.

2.3. Photopyhsical measurements

UV-vis and fluorescence spectroscopy were employed to study the photophysical properties of compound (**4**). The absorption and emission profiles were investigated in $1x10^{-6}$ M solutions of various solvents including tetrahydrofuran (THF), ethyl acetate (EA), dichloromethane (DCM), acetone (Ace), dimethylformamide (DMF), dimethyl sulfoxide (DMSO), acetonitrile (MeCN), ethanol (EtOH),

Celal Bayar University Journal of Science
Volume 20, Issue 3, 2024, p 100-105
Doi: 10.18466/cbayarfbe.1516889

methanol (MeOH), and n-hexane (n-Hex) (see Figure S7). Among these solvents, DMF was identified as the optimal choice due to its effective solubility for compound (**4**). Further investigation focused on DMF solutions, where absorption, emission and excitation spectra of compound (**4**) were recorded at a concentration of $1x10^{-6}$ M (see Figure 2). Additionally, solid-state absorption and emission spectra of compound (**4**) were examined (see Figure 3). The fluorescence quantum yield (Φ_F) of compound (**4**) was determined using the comparative method with a standard reference, 9,10-Diphenylanthracene (Φ_F = 0.95 in EtOH), according to Eq. (1) [32].

$$\Phi_F = \Phi_F(Std)\frac{F \cdot A_{Std} \cdot \eta^2}{F_{Std} \cdot A \cdot \eta^2_{Std}} \quad (1)$$

In this equation, Φ_F(Std) represents Φ_F of the reference molecule. F and F_{Std} denote the integrated areas under the fluorescence emission curves of compound (**4**) and the reference molecule, respectively. A and A_{Std} indicate the absorbances of compound (**4**) and the reference molecule at their respective excitation wavelengths. η^2 and η^2_{Std} are the squares of the refractive indices of the solvents for compound (**4**) and the reference molecule, respectively. The solutions of both compound (**4**) and the reference molecule were fixed at a concentration of $1x10^{-6}$ M for this measurement. Additionally, the fluorescence lifetime (τF) of compound (**4**) was directly measured and analyzed using a mono exponential calculation method.

3. Results and Discussion

3.1. Synthesis and Characterization

The fluorene derivative (**4**) was synthesized through a two-step reaction process outlined in Scheme 1. Initially, the dibromine derivative (**3**) was synthesized by reacting commercially available 9*H*-fluoren-9-one (**2**) with CBr_4 and PPh_3, following a procedure described in the literature (Fig. S5-S6) [31]. Subsequently, fluorene derivative (**4**) was obtained in high yield via a Suzuki coupling reaction between dibromide derivative (**3**) and 2.1 equivalents of (4-(diphenylamino)phenyl) boronic acid. The purity of compound (**4**) was confirmed through various analytical techniques including FT-IR, matrix-assisted MALDI-MS, ^{1}H NMR, ^{13}C NMR spectroscopy, and elemental analysis. Spectral data for compound (**4**) are provided in the Supplementary Information (Fig. S1-S4). All spectroscopic data corroborated the structure of compound (**4**). The FT-IR spectrum of compound (**4**) showed characteristic peaks indicative of its structure: aromatic =C-H stretches at 3055 and 3036 cm^{-1}, aromatic -C=C- stretch at 1586 cm^{-1}, and -C-N-C- stretch at 1273 cm^{-1} (Fig. S1). The molecular ion peak observed in the matrix-assisted MALDI-MS spectrum was 664.206 m/z, which closely matched the calculated value for compound (**4**) of 664.29 m/z (Fig. S2). In the ^{1}H NMR spectrum of compound (**4**), all expected aromatic proton signals appeared between 7.5-6.9 ppm (Fig. S3). Similarly, the ^{13}C NMR spectrum displayed aromatic carbon and quaternary carbon signals within the range of 150-115 ppm (Fig. S4). These spectroscopic analyses collectively confirmed the successful synthesis and structural integrity of compound (**4**).

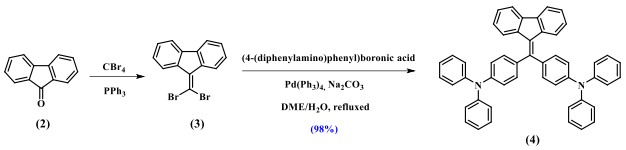

Scheme 1. Synthetic pathway of compound **(4)**.

3.2. Optical properties

Photophysical properties of compound (**4**) were thoroughly investigated in various solvents at a concentration of $1x10^{-6}$ M using UV-vis absorption and emission spectroscopy (Fig. S5). In DMF, the absorption spectrum of compound (**4**) displayed its maximum absorption band at 302 nm. Upon excitation at 340 nm, the emission spectrum showed a maximum emission band at 402 nm (Fig. 2). In the solid-state, compound (**4**) exhibited different absorption and emission characteristics compared to its DMF solution state (Fig. 3). Specifically, the emission wavelength shifted to 550 nm in the solid-state, indicating a red shift in emission compared to the 402 nm observed in DMF solution (Fig. 3b). This shift often indicates differences in molecular packing and environment between solution and solid phases. Φ_F of compound (**4**) was determined to be 0.78 in EtOH, using a comparative method with a standard reference (Fig. 4). Additionally, the τF of compound (**4**) was directly measured (Fig. 4). The τF value was determined through mono exponential calculations to be 1.7 ± 0.005 ns, representing the characteristic time scale of the fluorescence emission decay for the compound. These results provide a comprehensive understanding of the optical properties of compound (**4**), highlighting its behavior in different solvent environments and in solid-state conditions.

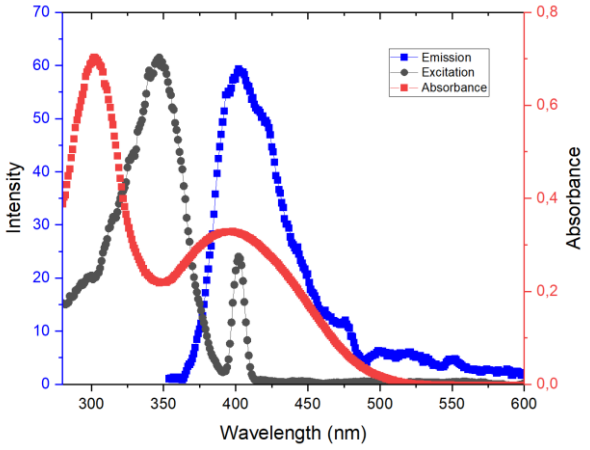

Figure 2. Absorption, emission and excitation spectra of compound (**4**) in DMF (λ_{exc}:340 nm).

Celal Bayar University Journal of Science
Volume 20, Issue 3, 2024, p 100-105
Doi: 10.18466/cbayarfbe.1516889

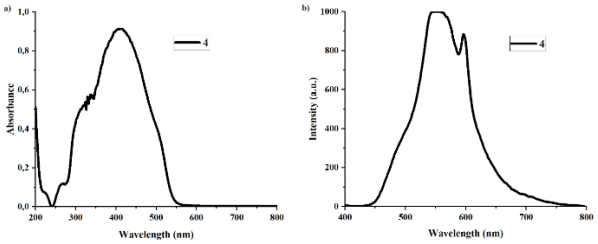

Figure 3. Solid-state **a)** absorption **b)** emission spectra of compound (**4**) (λ_{exc}:340 nm).

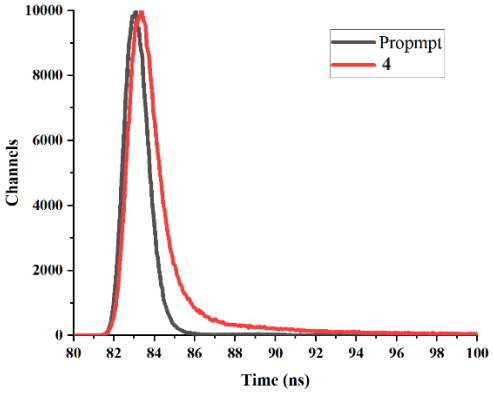

Figure 4. Fluorescence lifetime spectrum of compound (**4**).

3.3. Aggregation induced emission

Indeed, compound (**4**) demonstrates interesting photophysical properties, especially in mixed DMF-water solvent systems where the polarity and aggregation state can be tuned. Here's a breakdown of the observations: UV-vis Absorption Spectra (Figure 5a): In dilute DMF solution (1×10^{-6} M), compound (**4**) exhibits an absorption peak at 402 nm. As the fraction of water in the DMF-water mixture increases, the absorbance intensity gradually decreases. There is also a slight red shift observed in the absorption peak, particularly noticeable in the 50% DMF-water mixture. Fluorescence Emission Spectra (Figure 5b): The emission intensity of compound (**4**) remains weak when the water fraction is between 0% to 40% in the DMF-water mixture. Interestingly, at 50% water content, deteriorations in the emission profile start to appear, indicating possible aggregation effects. Additionally, an increase in the water fraction from 10% to 40% leads to a red shift in the emission wavelength by approximately 16 nm. These observations suggest that compound (**4**) exhibits significant AIE characteristics. The AIE effect is commonly observed in organic fluorophores where their emission intensity increases as they aggregate in the solid-state or in highly viscous environments, contrary to their behavior in dilute solutions where emissions are typically weaker due to non-radiative decay processes. In the case of compound (**4**), the presence of water in the DMF mixture seems to promote aggregation, leading to enhanced emission intensity and a shift in emission wavelength. These findings are crucial for understanding and potentially utilizing compound (**4**) in applications where controlled emission properties are desired, such as in sensing or imaging technologies.

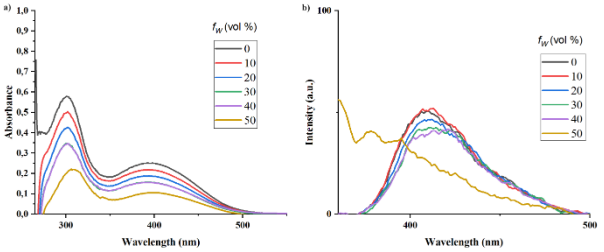

Figure 5. (a) Absorbance and b) emission spectra of dilute solutions of compound (**4**) ($1x10^{-6}$ M) in DMF-water mixtures with different water contents (0–50%). (λ_{exc}= 340 nm).

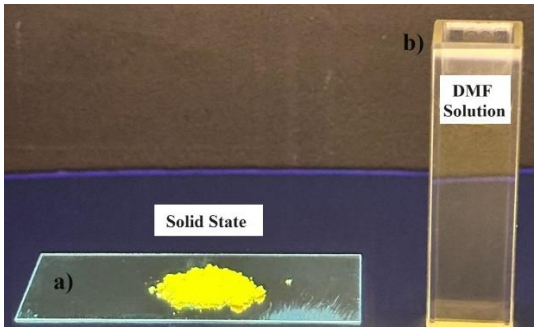

Figure 6. Photograph of a) solid-state sample and b) DMF solution of (**4**) under 365 nm UV illumination.

4. Conclusion

A novel electron-rich π-conjugated organic compound (**4**) featuring bis-TPA donor groups, and a fluorene core was successfully designed and synthesized in high yield through a two-step reaction process. The structural characterization of compound (**4**) was rigorously confirmed using FT-IR, MALDI-MS, ^{1}H NMR, ^{13}C NMR spectroscopy, and elemental analysis, all of which confirmed its structure accurately. We conducted a thorough investigation of photophysical features such as absorption, emission, excitation, and fluorescence lifetime using UV-vis and fluorescence spectroscopy instruments. Compound (**4**) exhibited bright yellow fluorescence in its solid-state form, indicating promising optical properties. Moreover, through studies of its AIE characteristics, it showed typical behavior where its emission intensity increased significantly in aggregated or solid-state environments compared to solution states. The strong solid-state emission characteristics of compound (**4**) suggest its potential for practical applications where intense and stable fluorescence is advantageous. Future studies will explore its mechano-chromic properties, further expanding its potential utility in responsive materials.

Author's Contributions

Seda Cetindere and Musa Erdoğan equally contributed to this manuscript, study conception, design, and synthesis. All authors read and approved the final manuscript.

Ethics

There are no ethical issues after the publication of this manuscript.

References

[1]. Zhao, Z, Lam, JWY, Tang, BZ. 2012. Tetraphenylethene: a versatile AIE building block for the construction of efficient luminescent materials for organic light emitting diodes. *J Mater Chem*; 22:23726-40.

[2]. Huang, J, Yang, X, Li, X, Chen, P, Tang, R, Li, F, Lu, P, Ma, Y, Wang, L, Qin, J, Li, Q, Li, Z. 2012. Bipolar AIE-active luminogens comprised of an oxadiazole core and terminal TPE moieties as a new type of host for doped electroluminescence. *Chem Commun;* 48: 9586-8.

[3]. Martinez-Manez, R, Sancenon, F. 2003. Fluorogenic and chromogenic chemosensors and reagents for anions. *Chem. Rev*; 103(11): 4419-4476.

[4]. Wang, M, Zhang, G, Zhang, D, Zhu, D, Tang, BZ. 2010. Fluorescent bio/chemosensors based on silole and tetraphenylethene luminogens with aggregation-induced emission feature. *J. Mater. Chem*; 20: 1858.

[5]. Yang, Y, Zhao, Q, Feng, W, Li, F. 2013. Luminescent chemodosimeters for bioimaging. *Chem. Rev*; 113: 192.

[6]. Zhang, Q, Yu, P, Fan, Y, Sun, C, He, H, Liu, X, Lu, L, Zhao, M, Zhang, H, Zhang, F. 2020. Bright and stable NIR-II J-aggregated AIE dibodipy-based fluorescent probe for dynamic in vivo bioimaging. *Angew. Chem., Int. Ed.;* 60: 3967.

[7]. Shimizu, M, Takeda, Y, Higashi, M, Hiyama, T. 2009. 1,4-Bis(alkenyl)-2,5-dipiperidinobenzenes: minimal fluorophores exhibiting highly efficient emission in the solid state. *Angew Chem Int Ed*; 48: 3653-6.

[8] Xue, P, Sun, J, Chen, P, Gong, P, Yao, B, Zhang, Z, Qian, C, Lu, R. 2015. Strong solid emission and mechanofluorochromism of carbazole-based terephthalate derivatives adjusted by alkyl chains. *J Mater Chem C*; 3: 4086-92.

[9]. Yuan, WZ, Lu, P, Chen, S, Lam, JW, Wang, Z, Liu, Y, Kwok, HS, Ma, Y, Tang, BZ. 2010. Changing the behavior of chromophores from aggregation-caused quenching to aggregation-induced emission: development of highly efficient light emitters in the solid state. *Adv Mater*; 22: 2159-63.

[10]. Domaille, DW, Que, EL, Chang, CJ. 2008. Synthetic fluorescent sensors for studying the cell biology of metals. *Nature Chemical Biology*; 4: 168–175.

[11]. Hong, YN, Lam, JWY, Tang, BZ. 2011. Aggregation-induced emission. *Chem. Soc. Rev*; 40: 5361–5388.

[12]. Hong, YN, Lam, JWY, Tang, BZ. 2009. Aggregation-induced emission: phenomenon, mechanism and applications. *Chem. Commun;* 4332-4353.

[13]. Kwok, RTK, Leung, CWT, Lam, JWY, Tang, BZ. 2015. *Chem. Soc. Rev*; 44: 4228–4238.

[14]. Mei, J, Hong, Y, Lam, JWY, Qin, A, Tang, Y, Tang, BZ. 2014. Aggregation-Induced Emission: The Whole Is More Brilliant than the Parts. *Adv. Mater*; 26: 5429–5479.

[15]. Luo, J, Xie, Z, Lam, JWY, Cheng, L, Chen, H, Qiu, C, Kwok, HS, Zhan, X, Liu, Y, Zhu, D, Tang, BZ. 2001. Aggregation-induced emission of 1-methyl-1,2,3,4,5-pentaphenylsilole. *Chem. Commun*; 1740–1741.

[16]. Kumbhar, HS, Shankarling, GS. 2015. Aggregation induced emission (AIE) active β-ketoiminate boron complexes: synthesis, photophysical and electrochemical properties. *Dyes Pigments*; 122: 85-93.

[17]. Kumar, M, Vij, V, Bhalla, V. 2012. Vapor-phase detection of trinitrotoluene by AIEE active hetero-oligophenylene-based carbazole derivatives. *Langmuir*; 28: 12417-21.

[18]. Shi, C, Guo, Z, Yan, Y, Zhu, S, Xie, Y, Zhao, YS, Zhu, W, Tian, H. 2013. Self-assembly solid-state enhanced red emission of quinolinemalononitrile: optical waveguides and stimuli response. *ACS Appl. Mater. Interfaces*; 5(1): 192-8.

[19]. Gu, X, Yao, J, Zhang, G, Zhang, C, Yan, Y, Zhao, Y, Zhang, D. 2013. New electron-donor/acceptor-substituted tetraphenylethylenes: aggregation-induced emission with tunable emission color and optical-waveguide behavior. *Chem Asian J*; 8(10): 2362-9.

[20]. Xu, F, Wang, H, Du, X, Wang, W, Wang, DE, Chen, S, Han, X, Li, N, Yuan, MS, Wang, J. 2016. Structure, property and mechanism study of fluorenone-based AIE dyes. *Dyes and Pigments;* 129: 121-128.

[21]. Du, X, Su, H, Zhao, L, Xing, X, Wang, B, Qiu, D, Wang, J, Yuan, MS. 2021. AIE-based donor–acceptor–donor fluorenone compound as multi-functional luminescence materials. *Mater. Chem. Front*; 5: 7508-7517.

[22]. Shaya, J, Corridon, PR, Al-Omari, B, Aoudi, A, Shunnar, A, Mohideen, MIH, Qurashi, A, Michel, BY, Burger, A. 2022. Design, photophysical properties, and applications of fluorene-based fluorophores in two-photon fluorescence bioimaging: A review. *Journal of Photochemistry and Photobiology C: Photochemistry Reviews*; 52, 100529.

[23]. Abbel, R, Schenning, APHJ, Meijer, EW. 2009. Fluorene-based materials and their supramolecular properties. *J. Polym. Sci. Part A: Polym. Chem*; 47: 4215–4233.

[24]. Moura, GLC, Simas, AM. 2010. Two-photon absorption by fluorene derivatives: systematic molecular design. *J. Phys. Chem. C*; 114(13): 6106–6116.

[25]. Kurdyukova, IV, Ishchenko AA. 2012. Organic dyes based on fluorene and its derivatives. *Russ. Chem. Rev;* 81: 258–290.

[26]. Ogawa, K. 2014. Two-photon absorbing molecules as potential materials for 3D optical memory. *Appl. Sci*; 4 (1): 1–18.

[27]. Lin, Y, Chen, Y, Ye, TL, Chen, ZK, Dai, YF, Ma, DG. 2012. Oligofluorene-based push–pull type functional materials for blue light-emitting diodes, *J. Photochem. Photobiol. A: Chem;* 230(1): 55-64.

[28]. Lim, K, Kim, C, Song, J, Yu, T, Lim, W, Song, K, Wang, P, Zu, N, Ko, J. 2011. Enhancing the performance of organic dye-sensitized solar cells via a slight structure modification. *J. Phys. Chem. C;* 115: 22640–22646.

[29]. Erdoğan, M, Horoz, S. 2021. Synthesis and characterization of a triphenylamine-dibenzosuberenone-based conjugated organic material and an investigation of its photovoltaic properties. *Journal of Chemical Research*; 45(1-2): 207-212.

[30]. Erdoğan, M, Orhan, Z, Daş, E. 2022. Synthesis of electron-rich thiophene triphenylamine based organic material for photodiode applications. *Optical Materials*; 128:12446.

[31]. Chen, ZQ, Chen, T, Liu, JX, Zhang, GF, Li, C, Gong, WL, Xiong ZJ, Xie, NH, Tang, BZ, Zhu, MQ. 2015. Geminal cross-coupling of 1, 1-dibromoolefins facilitating multiple topological π-conjugated tetraarylethenes. *Macromolecules*; 48(21): 7823-7835.

[32]. Yildirim-Sarikaya, S, Ardic-Alidagi, H, Cetindere, S. 2023. Novel BODIPY-Fluorene-Fullerene and BODIPY-Fluorene-BODIPY Conjugates: Synthesis, Characterization, Photophysical and Photochemical Properties. *Journal of Fluorescence*; 33: 297–304.

[33]. Tan, S, Yin, Y, Chen, W, Chen, Z, Tian, W, Pu, S. 2020. Carbazole-based highly solid-state emissive fluorene derivatives with various mechanochromic fluorescence characteristics. *Dyes and Pigments*; 177: 108302.

[34]. Chen, Z, Liang, J, Han, X, Yin, J, Yu, GA, Liu, SH. 2015. Fluorene-based novel highly emissive fluorescent molecules with aggregate fluorescence change or aggregation-induced emission enhancement characteristics. *Dyes and Pigments*; 112: 59-66.

[35]. Gouthaman, S, Jayaraj, A, Sugunalakshmi, M, Sivaraman, G, Swamy, PCA. 2022. Supramolecular self-assembly mediated aggregation-induced emission of fluorene-derived cyanostilbenes: multifunctional probes for live cell-imaging. *J. Mater. Chem. B*; 10: 2238.

[36]. Zhou, X, Li, H, Chi, Z, Zhang, X, Zhang, J, Xu, B, Zhang, Y, Liu, S, Xu, J. 2012. Piezofluorochromism and morphology of a new aggregation-inducedemission compound derived from tetraphenylethylene and carbazole. *New. J. Chem*; 36: 685–693.

[37]. Dong, YQ, Lam, JWY, Qin, AJ, Sun, JX, Liu, JZ, Li, Z, Sun, JZ, Sung, HHY, Williams, ID, Kwok, HS, Tang, BZ. 2007. Aggregation-induced andcrystallization-enhanced emissions of 1,2-diphenyl-3,4-bis(diphenylmethylene)-1-cyclobutene. *Chem. Commun*; 3255–3257.

[38]. Duraimurugan, K, Balasaravanan, R, Siva, A. 2016. Electron rich triphenylamine derivatives (D-π-D) for selective sensing of picric acid in aqueous media. *Sensors and Actuators B*; 231: 302–312.